



HAL
open science

Energy Planning for Unmanned Over-Actuated Road Vehicle

Ismail Bensekrane, Pushendra Kumar, Achille Melingui, Vincent Coelen,
Yacine Amara, Rochdi Merzouki

► **To cite this version:**

Ismail Bensekrane, Pushendra Kumar, Achille Melingui, Vincent Coelen, Yacine Amara, et al.. Energy Planning for Unmanned Over-Actuated Road Vehicle. 2018 IEEE Vehicle Power and Propulsion Conference (VPPC), Aug 2018, Chicago, United States. pp.1-6, 10.1109/VPPC.2018.8604990 . hal-02053362

HAL Id: hal-02053362

<https://hal.science/hal-02053362>

Submitted on 1 Mar 2019

HAL is a multi-disciplinary open access archive for the deposit and dissemination of scientific research documents, whether they are published or not. The documents may come from teaching and research institutions in France or abroad, or from public or private research centers.

L'archive ouverte pluridisciplinaire **HAL**, est destinée au dépôt et à la diffusion de documents scientifiques de niveau recherche, publiés ou non, émanant des établissements d'enseignement et de recherche français ou étrangers, des laboratoires publics ou privés.

Energy Planning for Unmanned Over-actuated Road Vehicle

Ismail Bensekrane¹ Pushpendra Kumar¹ Achille Melingui² Vincent Coelen¹ Yacine Amara³ Rochdi Merzouki¹

Abstract—Energy planning for unmanned road vehicles (URVs) is an important step for the management of the autonomous driving. This energy planning depends on the model for power consumption estimation related to URVs. Generally URVs are over-actuated, and this property leads to multiple kinematic configurations for driving. Consequently, it adds more constraints and more complexity for energy planning. In this paper, a Neuro-Fuzzy model is developed for power consumption estimation for different driving modes configurations of URV. Furthermore, a dynamic programming algorithm is applied to find the optimal velocity profile, and the optimal configuration mode in each segment of the road for an over-actuated URV called RobuCAR, used for experimental validation.

Index Terms—Power consumption estimation, Energy planning management, Neuro-Fuzzy modeling, Dynamic programming.

I. INTRODUCTION

A. Power Consumption by URV

The power consumption estimation is mainly related to the URV's dynamic parameters. Battery Management System (BMS) [1] is used to monitor instantly the electric power of batteries for vehicles. Energy Management Strategy (EMS) is used to identify the energy optimal control of an over-actuated vehicle [2], to maximize the traveling distance [3]. Both BMS and EMS cannot estimate the instantaneous power consumption of an URV during the trajectory tracking under kinematic and dynamic conditions of driving. The kinematic parameters are essentially represented by the degree of actuation redundancy, degree of steerability, and the road geometry in terms of path curvature [4].

The development of a model of power consumption is often elaborated using a linear regression model or exponential logarithmic model [5], [6]. Generally, those models can not represent with accuracy due to presence of non-linearities and not considering the driving modes of navigation and road curvature. In [4], a model is presented taking into account the path curvature C , degree of steerability δ_S , and degree of actuation redundancy δ_R , to estimate analytically power consumption. But, analytical models cannot model all the system non-linearities and complexities. Therefore, it is

required to look for new methods with better accuracy as Neural network and Adaptive Neuro Fuzzy Inference System (ANFIS) [7].

Neural network modeling is among many types of modeling methods with better accuracy, and often used to characterize a nonlinear system. Many models have been developed for the power consumption estimation for electric or hybrid vehicles using neural network. In [8], a neural network based prediction of energy consumption is developed for an electric vehicle considering the driving style of driver. Sakayori et al. [9] used multilayer perception (MLP) neural network to predict power consumption for an autonomous mobile robot, including the slope, heading angle, and velocity profile as inputs. Masikos et al. [10] presented a MLP neural network for an electric vehicle to predict the energy consumption in urban area with a 10% of average accuracy. In [11], neural network is used to estimate torque and brake fuel specific consumption (BFSC) for the gasoline engine. The limitation of these works is the high percentage of average error, which can not be appropriate for autonomous navigation of an over-actuated URV. Furthermore, these works have not considered many possible driving modes configurations of an over-actuated URV. [7] find that ANFIS present better performances than Neural network modeling. In this work ANFIS is considered to estimate the instantaneous power consumption for different driving mode configurations of URV.

B. Energy Planning Management

In addition to power consumption estimation modeling, it is important to have a good strategy for energy planning management. The main objective of energy planning management is to optimize energy consumption by URV for a given trip. Many researchers developed energy optimization strategies using dynamic programming ([12],[13]). Moreover, authors developed energy optimization methods using model predictive control (MPC) and compared with dynamic programming based methods([3],[14]). Furthermore, the power management has been studied by using control allocation for over-actuated URV based on parametric torque distribution [15]. But, this approach considered only dynamics of the vehicle and not the road profile. Chen et al. [3] estimated the optimal velocity profile and torque using dynamic programming method for an URV considering its front steering. In [16], neural network and MPC based method is developed for energy optimization and compared with dynamic programming algorithm. In [17], quadratic programming is used to develop energy optimization for

¹ Polytech Lille, CRIStAL, CNRS-UMR 9189, Avenue Paul Langevin, 59655 Villeneuve d'Ascq, France
ismail.bensekrane@polytech-lille.fr
rochdi.merzouki@polytech-lille.fr
Vincent.Coelen@polytech-lille.net
jahan.pushp@gmail.com

² Université de Yaoundé1, Cameroun
achillemelingui@gmail.com

³ Ecole Militaire Polytechnique, Algérie
amara.yacine@gmail.com

URV. In this paper, we are applying a dynamic programming algorithm to find the optimal velocity profile and the optimal driving mode in each segment of the trajectory.

C. Problem Statements and Contribution

Based on the above literature review, we found that not much models are available for power consumption estimation by an URV, in addition, analytical models can not provide precise results due to non-linearities of the system and parametric uncertainties. Moreover, existing methods of energy planning consider optimization of velocity profile for a given trajectory, but optimization of different driving modes have not been considered. In this paper, a model for power consumption estimation is developed using Neuro-fuzzy approach for minimizing the modeling errors. Furthermore, a dynamic programming is developed for energy planning management of an URV, which optimizes the velocity profile and the driving mode for each section of a given trajectory (Fig. 1).

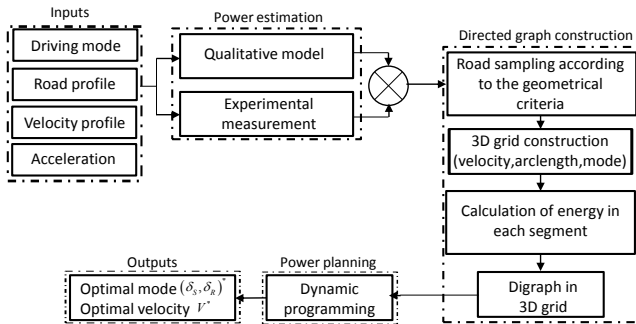


Fig. 1: The proposed methodology for power consumption estimation and energy planning management.

In Fig. 1, power is estimated for an URV using a qualitative model (ANFIS), which is compared with the experimental measurements of power consumption obtained from a professional real-time simulation software for vehicle dynamics used by automotive industries namely, SCANr Studio [18]. The inputs to model are driving mode, road profile (curvature of the trajectory), velocity profile, and acceleration for a given trajectory. In the next step, a directed graph is generated to apply the optimization method. For this, road sampling is performed to obtain different segments of it based on curvature of the road considering three types of road segments i.e., line, clothoid, and arc. Then, a 3D grid is constructed with three axes of velocity, arclength of the segment, and driving mode; the purpose of using 3D grid is to consider different driving modes on a third axis, which is not possible with a 2D grid [12]. In this grid, all the feasible points for each driving mode are given. Then, total energy consumption in each segment of the road are calculated, which are weights of digraph edges. Finally, digraph is constructed in the 3D grid, where nodes represent starting and ending points for the different segments of the road profile. Dynamic programming is applied on the digraph to find the optimal global solution in terms of optimal velocity



Fig. 2: RobuCAR

and optimal driving mode for each segment of the road profile.

D. Paper Organization

The remaining paper is organized in the following sections. In Section II, power consumption model of an URV is developed. In section III, the energy planning management algorithm is developed. Section IV discusses about simulation results. Section VI concludes this paper with a summary of our observations.

II. POWER CONSUMPTION ESTIMATION

In this section, Neuro-fuzzy model is developed for the power consumption estimation of a four wheeled over-actuated URV. The model considers the degree of actuation redundancy δ_R , degree of steerability δ_S , and the path curvature C ; for definition of these terms one can refer to [4].

In this paper, we analyze a four wheeled URV called RobuCAR (Fig. 2). RobuCAR is a four wheeled autonomous vehicle with on-board computer and electronics. The four wheels are independently driven by DC motors. There are two steering control systems for the steering of front and rear wheels. There are total six input actuators (traction and steering) to control its motion in a plane with three degrees of freedom (DoF) i.e., longitudinal, lateral, and yaw motions; therefore, RobuCAR is an over-actuated URV. Moreover, it is a non-holonomic URV because it cannot move in the three DoF without steering. According to δ_S and δ_R , RobuCAR can have different possible driving modes configurations as shown in Fig. 3.

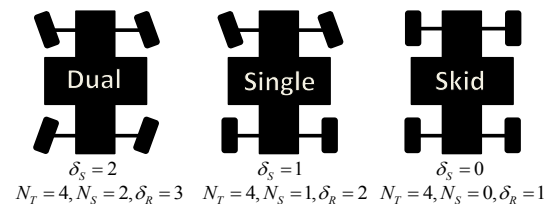


Fig. 3: Different types of configuration of RobuCAR

Refer to Fig. 3, N_T and N_S denote total number of active traction and steering actuators in a configuration, respectively. The Dual configuration ($\delta_S = 2$) has two steering

control systems for the steering of front and rear wheels. In the Single configuration ($\delta_S = 1$), there is only one steering control system for the steering of front wheels. The Skid configuration ($\delta_S = 0$) has no steering system, and all the four wheels are the fixed tractive wheels. We represented three configuration with a number 4, which denotes that all the four wheels are tractive. In addition, δ_R for each configuration is shown in Fig. 3, it can be observed that δ_R depends on δ_S .

A. Adaptive neuro fuzzy inference system (ANFIS)

ANFIS have been successfully used for approximation tasks [19], [20]. In this paper, ANFIS is used to estimate power consumption of an URV. The ideal may be to build an ANFIS model which emulates the different URV actuation modes. However, as we will see in the simulation results, the URV behavior from one actuation mode to another is so different that three separate ANFIS models, one for each actuation mode, have been built to improve regression performance. In the following subsections the ANFIS structure and the learning algorithm are presented.

1) *ANFIS structure:* The ANFIS structure considered in this work is shown in Fig. 4. The inputs to ANFIS model are curvature of the road C , velocity V and acceleration A of the URV, while power consumed by URV is the output of the ANFIS model. Takagi and Sugeno's type rules are considered [19] as follows:

Rule1: If C is C_1 and V is V_1 and A is A_1 , then P_ω is $p_1C + q_1V + r_1A + s_1$.

Where, p_1 , q_1 , r_1 , and s_1 are constants, while, V_1 , A_1 , and C_1 , are the fuzzy sets in the antecedents, and $P_\omega = f(C, V, A)$ is a crisp function in the consequent.

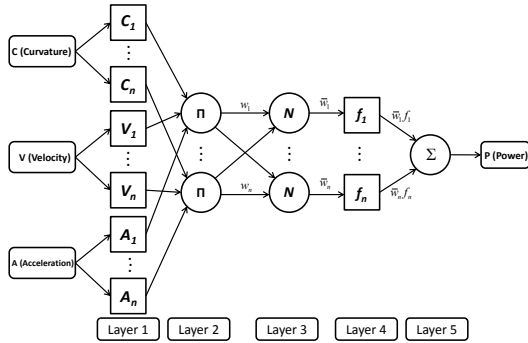


Fig. 4: ANFIS structure for one driving mode

The output of each ANFIS layer is evaluated as follows:

Layer 1: Each i^{th} node in this layer is given by:

$$O_i^1 = \mu_{A_i}(x) \quad (1)$$

where, x is the input to i^{th} node, A_i is the linguistic variable associated with this node function, and μ_{A_i} is the membership function of A_i . The generalized bell-shaped membership function is chosen for $\mu_{A_i}(x)$:

$$\mu_{A_i}(x) = \frac{1}{1 + \left[\frac{(x - c_i/a_i)^2}{b_i} \right]} \quad (2)$$

where, $\{a_i, b_i, c_i\}$ is the premise parameter set.

Layer 2: Each node in this layer calculates the firing strength w_i of a rule. The output of each node is the product of all the incoming signals to it:

$$O_i^2 = w_i = \mu_{C_i}(C) \times \mu_{V_i}(V) \times \mu_{A_i}(A), \quad i = 1, 2, \dots, n. \quad (3)$$

Layer 3: The output of each node is the normalized firing strength given by:

$$O_i^3 = \bar{w}_i = \frac{w_i}{w_1 + w_2 + \dots + w_n} \quad (4)$$

Layer 4: Every i^{th} node in this layer is an adaptive node with a node function given by:

$$O_i^4 = \bar{w}_i f_i = \bar{w}_i (p_i C + q_i V + r_i A + s_i) \quad (5)$$

where, \bar{w}_i is the output of Layer 3 and $\{p_i, q_i, r_i, s_i\}$ is the consequent parameter set.

Layer 5: This layer comprises one node, and computes the overall output as the summation of all incoming signals, i.e.,

$$O_i^5 = \text{overall output} = \sum_i \bar{w}_i f_i = \frac{\sum_i w_i f_i}{\sum_i w_i} \quad (6)$$

2) *Learning algorithm:* By observing the ANFIS structure, it can be observed that the values of the premise parameters and the output of the system can be expressed as a linear combination of the consequent parameters ($p_1, q_1, r_1, s_1, \dots, p_n, q_n, r_n, s_n$).

$$\begin{aligned} f &= \frac{w_1}{w_1 + w_2 + \dots + w_n} f_1 + \frac{w_2}{w_1 + w_2 + \dots + w_n} f_2 + \dots \\ &+ \frac{w_n}{w_1 + w_2 + \dots + w_n} f_n \\ &= \bar{w}_1 f_1 + \bar{w}_2 f_2 + \dots + \bar{w}_n f_n \\ &= (\bar{w}_1 C) p_1 + (\bar{w}_1 V) q_1 + (\bar{w}_1 A) r_1 + (\bar{w}_1) s_1 + (\bar{w}_2 C) p_2 \\ &+ (\bar{w}_2 V) q_2 + (\bar{w}_2 A) r_2 + (\bar{w}_2) s_1 + \dots + (\bar{w}_n C) p_n \\ &+ (\bar{w}_n V) q_n + (\bar{w}_n A) r_n + (\bar{w}_n) s_n \end{aligned} \quad (7)$$

In the learning process, the consequent parameters are identified by using the least squares estimate in the forward pass. In the backward pass, the premise parameters are updated by mean of the gradient descent algorithm using the error signals [19].

3) *Learning and validation of ANFIS models:* The database for ANFIS model learning is built by using the engineering software SCANer studio.

Different training paths containing data of the curvature points in the vehicle's trajectory are considered. In SCANer studio environment, the velocity profile in range [1, 16] km/h with a step size of 1 km/h is used for each driving mode; the velocity profile, acceleration, path curvature, and the consumed power are recorded. We obtained the databases of 262079, 264634, and 400965 samples respectively for, Dual mode, Single mode, and Skid mode. Each database is divided into three subsets: training, validation and test sets. The training set is used during the learning phase, and the test set is only used to evaluate the performance of ANFIS

models. For a good generalization and to avoid over-fitting, the validation set is used during the training phase and the early-stopping method is applied for training. The early-stopping method requires that after a period of training (an epoch) using the training set, the weight matrices of ANFIS are fixed, and the ANFIS operates in the forward mode using the validation set. The process is reiterated until the mean square error (MSE) on the validation set reaches its minimum value.

For ANFIS parameters initialization, three membership functions are considered for each linguistic variable, and the grid partitioning method is used to initialize the fuzzy rules, the premise and consequent parameters. The different ANFIS models converge approximately after 2000 epochs. The following MSE, $2.56e^{-3}$, $2.27e^{-3}$, $3.03e^{-2}$ respectively for, Dual mode, Single mode, and Skid mode are obtained on the corresponding test sets.

In Fig. 5(a,c,e), a comparison of power consumption of the URV using ANFIS and SCANer is given for Skid, Single, and Dual configurations, respectively. The errors between these models are shown in Fig. 5(b,d,f).

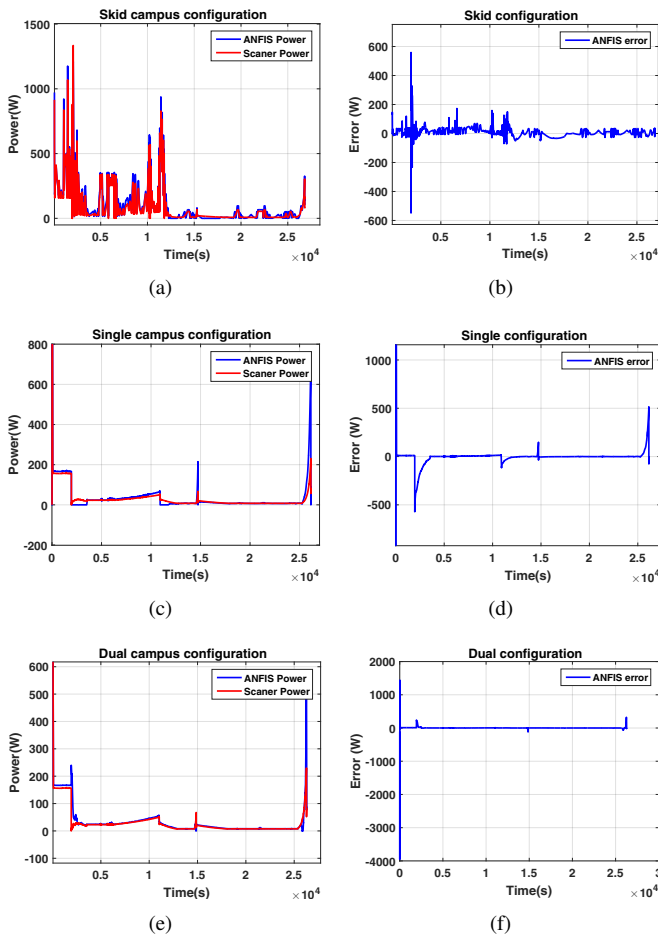


Fig. 5: Power estimation

From the results, it can be observed that ANFIS model follows almost the same profile as SCANer. However, there

are peaks of errors at some points due to turns in the trajectory.

III. ENERGY PLANNING MANAGEMENT

The energy planning strategy considers the dynamics of URV and the road geometry for each segment of the planned trajectory. To reach this goal, a cost function is given to minimize.

$$\min_{V,M} J = \sum_{i=1}^n E_k(t_i, V_i, C_i, M_{i,k}) \quad (8)$$

s.t.

$$\begin{aligned} V_{\min} &\leq V_i \leq V_{\max} \\ T_{\min} &\leq T_i \leq T_{\max} \\ a_{\min} &\leq a_i \leq a_{\max} \end{aligned} \quad (9)$$

$$E_k(s_i, V_i, C_i, M_{i,k}) = \int_k^{k+1} P_k dt \quad (10)$$

$$M_{i,k} = \begin{cases} \delta_s = 0, \delta_R = 1 & \text{Skid(Over-actuated)} \\ \delta_s = 1, \delta_R = 2 & \text{Single(Over-actuated)} \\ \delta_s = 2, \delta_R = 3 & \text{Dual(Over-actuated)} \end{cases} \quad (11)$$

Where, E_k and P_k represent energy consumed and instantaneous power consumption for the k th configuration of URV, respectively. The parameters t_i , V_i , and C_i represent traveling time, actual velocity, and curvature in i th segment, respectively. T_i represents the total torque for the four wheel drive configuration with lower and upper limits T_{\min} and T_{\max} , respectively.

a_i represents the total acceleration for the four wheel drive configuration with lower and upper limits a_{\min} and a_{\max} , respectively.

A. Road Profile

In a Geographical Information System (GIS), a road is represented by polylines [21], describing the central axis of its surface. The road path is decomposed into horizontal and vertical curves representing respectively the roads mapped onto the plane (Fig. 6(a)). In this paper, we use the cubic spline interpolation approach for polylines describing the considered trajectory [22].

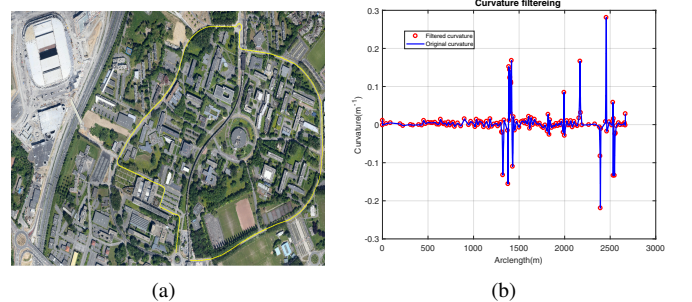


Fig. 6: (a) Campus trajectory of the University of Lille and (b) the filtered and real curvature

B. Trajectory Filtering

The GIS data for real road is often tainted by errors of acquisition systems, which explains the fluctuations presented in the estimated curvature of the 2D trajectory. The curvature of the trajectory can take three forms:

$$C_i = \begin{cases} 0 & \text{Straight line} \\ \text{Constant} & \text{Arc} \\ as + b & \text{Clothoide} \end{cases} \quad (12)$$

where, s represents the arc length; while a and b are constant parameters of clothoide in $C-s$ plane. The estimated and filtered curvature for the campus of university of Lille 1 is shown in Fig. 6 (b) ($C-s$ plane), with total of 138 segments.

In each segment of the trajectory, a unique drive pattern is applied (acceleration, constant velocity, or deceleration) as shown in Fig.7. In addition, it is considered that each segment (line, clothoid, and arc) has constraint of driving mode, which are detailed in Table I.

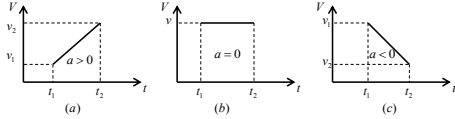


Fig. 7: Driving pattern during sampling intervals

TABLE I: Driving mode constraints

	Line $c = 0$	Clothoid $c = var$	Arc $c = cst$
Skid ($\delta_s = 0, \delta_R = 1$)	X	X	X
Single ($\delta_s = 1, \delta_R = 2$)		X	X
Dual ($\delta_s = 2, \delta_R = 3$)		X	X

C. Dynamic Programming

To solve the non-linear problem of energy planning, we apply dynamic programming algorithm on weighted digraph.

1) *3D grid construction*: The grid consists of 3 axes, arclength which is represented with a set of samples of distance $d = \{d_0, d_1, d_2, \dots, d_n\}$, velocity $v = \{v_{min} : \Delta v : v_{max}\}$, and driving mode $m = \{Skid, Dual, Single\}$. Each point in the grid is obtained with respect to all constraints namely, geometrical, kinematic, and dynamic such as velocity, acceleration, and torque; as shown in Fig. 8. In this approach, arclength is segmented according to the geometrical criteria, which is usually non uniform segmentation.

2) *Digraph construction*: A digraph is a weighted directed graph, where the edges have a direction associated with them. A directed graph is an ordered pair $G = (Ve, Ed)$, where Ve is a set of vertices representing end points of each segment and Ed is a set of edges representing connection between vertices as a function of velocity, mode, and arclength. The weight on each edge represents energy consumed to travel the corresponding segment for each mode.

Each vertex is denoted with a specific number say, jkl , where j , k , and l represent j th row of velocity vector, k th row of mode vector, and l th row of segment vector, respectively. In addition, a starting and an ending vertex is added on the

top and the bottom of the digraph. The starting vertex is connected to the first set of vertices with zero weights on edges. Similarly, the ending vertex is connected to the last set of vertices with zero weights on edges.

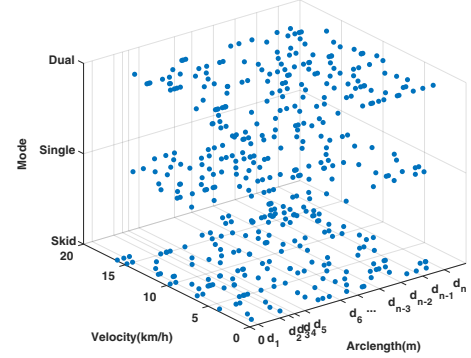


Fig. 8: Schematic of 3D grid construction

The developed digraph is used to find shortest path between the starting and the ending points by applying dynamic programming.

IV. SIMULATION BASED ON EXPERIMENTAL DATA

A set of experimental data from embedded sensors of the RoboCAR during its autonomous driving along the trajectory of Fig. 6(a) are collected for three kinematic configurations. These data are then used for power consumption estimation and energy planning for the driving management.

In Fig. 9 and 10, the optimal velocity profile (4-16 km/h) and the optimal configuration modes are presented for each segment of the filtered trajectory in $s-V$ and $X-Y$ planes, respectively. The algorithm shows that Single mode is the most optimal for the given optimal velocity profile as shown in Fig. 11. The Dual mode should be used in sharp turns and Skid mode in some line segments along the trajectory. Furthermore, the energy consumption for each driving mode is given in Table II, while considering only one mode for the whole trajectory tracking. From the Table II, it can be observed that the proposed optimal driving strategy with changing driving modes consumes less energy in comparison to the one mode driving.

TABLE II: Comparison of energy consumption

	Energy consumption (J)
Skid for optimal velocity	3.1573e+06
Single for optimal velocity	3.0279e+05
Dual for optimal velocity	4.5242e+05
Optimal modes and optimal velocity	1.6912e+04

V. CONCLUSION

This paper presents a method of energy planning of an over-actuated URV based on power consumption estimation model. The power consumption is estimated using a qualitative ANFIS model for different configuration modes of an URV called RobuCAR. Dynamic programming algorithm

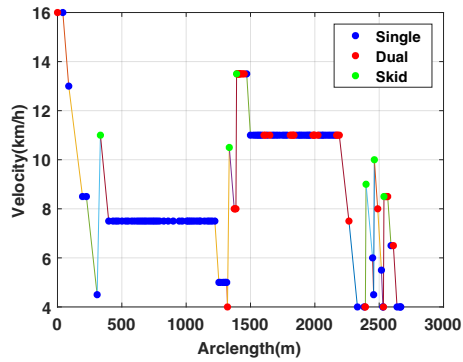


Fig. 9: Optimal velocity profile and optimal modes in each segment of the trajectory ($s - V$ plane)

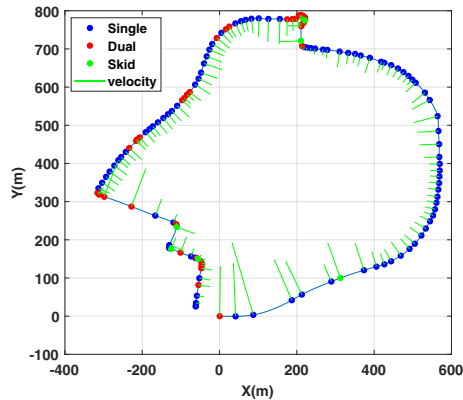


Fig. 10: Optimal velocity profile and optimal modes in each segment of the trajectory ($X - Y$ plane)

is applied to obtain the global optimal velocity profile and the optimal driving mode associated with each segment of the trajectory in off-line mode. The combinations of optimal driving modes and optimal velocity gives optimal energy consumption for the whole trajectory tracking in comparison to one mode driving. For future work, an extension to the case of faulty actuator will be considered for the energy planning strategy.

REFERENCES

- [1] A. Szumanowski and Y. Chang, "Battery management system based on battery nonlinear dynamics modeling," *IEEE Transactions on Vehicular Technology*, vol. 57, no. 3, pp. 1425–1432, May 2008.
- [2] J. Brembeck and P. Ritzer, "Energy optimal control of an over actuated robotic electric vehicle using enhanced control allocation approaches," in *2012 IEEE Intelligent Vehicles Symposium*, June 2012, pp. 322–327.
- [3] Y. Chen, X. Li, C. Wiet, and J. Wang, "Energy management and driving strategy for in-wheel motor electric ground vehicles with terrain profile preview," *IEEE Transactions on Industrial Informatics*, vol. 10, no. 3, pp. 1938–1947, Aug 2014.
- [4] I. Bensekrane, P. Kumar, Y. Amara, and R. Merzouki, "Towards adaptive power consumption estimation for over-actuated unmanned vehicles," in *Robotics and Biomimetics (ROBIO), 2017 IEEE International Conference on*. IEEE, 2017, pp. 92–97.
- [5] S. Dogru and L. Marques, "Power characterization of a skid-steered mobile field robot," in *2016 International Conference on Autonomous Robot Systems and Competitions (ICARSC)*, May 2016, pp. 15–20.

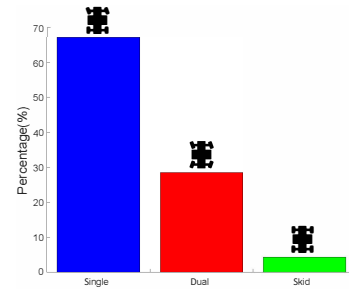


Fig. 11: Percentage of modes use in campus trajectory

- [6] O. Chuy, E. G. Collins, W. Yu, and C. Ordenez, "Power modeling of a skid steered wheeled robotic ground vehicle," in *2009 IEEE International Conference on Robotics and Automation*, May 2009, pp. 4118–4123.
- [7] M. Bilgehan, "Comparison of anfis and nn models with a study in critical buckling load estimation," *Applied Soft Computing*, vol. 11, no. 4, pp. 3779–3791, 2011.
- [8] J. Felipe, J. C. Amarillo, J. E. Naranjo, F. Serradilla, and A. Daz, "Energy consumption estimation in electric vehicles considering driving style," in *2015 IEEE 18th International Conference on Intelligent Transportation Systems*, Sept 2015, pp. 101–106.
- [9] G. Sakayori and G. Ishigami, "Energy efficient slope traversability planning for mobile robot in loose soil," in *2017 IEEE International Conference on Mechatronics (ICM)*, Feb 2017, pp. 99–104.
- [10] M. Masikos, K. Demestichas, E. Adamopoulou, and M. Theologou, "Reliable vehicular consumption prediction based on machine learning," *Neural Network World*, vol. 24, no. 4, p. 333, 2014.
- [11] N. K. Togun and S. Baysec, "Prediction of torque and specific fuel consumption of a gasoline engine by using artificial neural networks," *Applied Energy*, vol. 87, no. 1, pp. 349–355, 2010.
- [12] E. Ozatay, S. Onori, J. Wollaeger, U. Ozguner, G. Rizzoni, D. Filev, J. Michelini, and S. D. Cairano, "Cloud-based velocity profile optimization for everyday driving: A dynamic-programming-based solution," *IEEE Transactions on Intelligent Transportation Systems*, vol. 15, no. 6, pp. 2491–2505, Dec 2014.
- [13] C. Zhang, A. Vahidi, P. Pisu, X. Li, and K. Tennant, "Role of terrain preview in energy management of hybrid electric vehicles," *IEEE Transactions on Vehicular Technology*, vol. 59, no. 3, pp. 1139–1147, March 2010.
- [14] D. Quaglia and R. Muradore, "Communication-aware bandwidth-optimized predictive control of motor drives in electric vehicles," *IEEE Transactions on Industrial Electronics*, vol. 63, no. 9, pp. 5602–5611, 2016.
- [15] A. M. Dizqah, B. Lenzo, A. Sormiotti, P. Gruber, S. Fallah, and J. D. Smet, "A fast and parametric torque distribution strategy for four-wheel-drive energy-efficient electric vehicles," *IEEE Transactions on Industrial Electronics*, vol. 63, no. 7, pp. 4367–4376, July 2016.
- [16] C. Zhang, S. Zhang, G. Han, and H. Liu, "Power management comparison for a dual-motor-propulsion system used in a battery electric bus," *IEEE Transactions on Industrial Electronics*, vol. 64, no. 5, pp. 3873–3882, May 2017.
- [17] W. Liu, A. Khajepour, H. He, H. Wang, and Y. Huang, "Integrated torque vectoring control for a three-axle electric bus based on holistic cornering control method," *IEEE Transactions on Vehicular Technology*, vol. PP, no. 99, pp. 1–1, 2017.
- [18] "Oktal website for scanner studio," <http://www.oktal.fr/en/>.
- [19] J.-S. Jang, "Anfis: adaptive-network-based fuzzy inference system," *IEEE transactions on systems, man, and cybernetics*, vol. 23, no. 3, pp. 665–685, 1993.
- [20] M. Buragohain and C. Mahanta, "A novel approach for anfis modelling based on full factorial design," *Applied soft computing*, vol. 8, no. 1, pp. 609–625, 2008.
- [21] S. Jakkula, Y. Shen, and J. Sokolowski, "Extraction of road network topology for transportation and gis applications," in *MODSIM World Conference & Expo Virginia Beach, VA, 2007*.
- [22] J. H. Ahlberg, E. N. Nilson, and J. L. Walsh, "The theory of splines and their application," 1967.